horticulturae

MDPI

Article

AquaCrop Model Performance in Yield, Biomass, and Water Requirement Simulations of Common Bean Grown under Different Irrigation Treatments and Sowing Periods

Ružica Stričević *, Aleksa Lipovac, Nevenka Djurović, Dunja Sotonica and Marija Ćosić

Faculty of Agriculture, University of Belgrade, Nemanjina 6, 11080 Zemun, Serbia; alipovac@agrif.bg.ac.rs (A.L.); marasn@agrif.bg.ac.rs (N.D.); dunja.sotonica@agrif.bg.ac.rs (D.S.); c.marija@agrif.bg.ac.rs (M.Ć.)
* Correspondence: sruzica@agrif.bg.ac.rs

Abstract: The application of crop growth simulation and water management models will become increasingly important in the future. They can be used to predict yield reductions due to water scarcity and allocate water to ensure profitable crop production. The objective of this research was to calibrate the AquaCrop model for common bean (*Faseolus vulgaris* L.) grown in temperate climates and to test whether the model can be used for different irrigation strategies to achieve high yield productivity. The model was calibrated using data obtained from two years of experimental research in the Serbian territory of the Syrmia region. There were three sowing periods/plots: I—mid April, II—end of May/beginning of June, and III—third decade of June/beginning of July; and three levels of irrigation/subplots: full irrigation (F) providing 100% of crop evapotranspiration (ETc), mild deficit irrigation (R) at 80% of ETc, and moderate deficit irrigation (S) at 60% of ETc. The results show that the AquaCrop model accurately predicts common bean yield, biomass, canopy cover, and water requirements. The statistical indices of the calibrated dataset, coefficient of determination (R^2), normalized root mean square error (*NRMSE*), mean bias error (*MBE*), and Willmott agreement index (*d*) for yield and biomass were: 0.91, 0.99; 6.9%, 11.4%; −0.046, 1.186 and 0.9, 0.89, respectively. When testing three irrigation strategies, the model accurately predicted irrigation requirements for the full and two deficit irrigation strategies, with only 29 mm, 32 mm, and 34 mm more water than was applied for the Fs, Rs, and Ss irrigation strategy, respectively. The AquaCrop model performed well in predicting irrigated yield and can be used to estimate the yield of common bean for different sowing periods and irrigation strategies.

Keywords: common bean; irrigation strategy; AquaCrop; sowing periods; canopy cover

check for updates

Citation: Stričević, R.; Lipovac, A.; Djurović, N.; Sotonica, D.; Ćosić, M. AquaCrop Model Performance in Yield, Biomass, and Water Requirement Simulations of Common Bean Grown under Different Irrigation Treatments and Sowing Periods. *Horticulturae* **2023**, *9*, 507. https://doi.org/10.3390/horticulturae9040507

Academic Editor: Arturo Alvino

Received: 13 March 2023
Revised: 11 April 2023
Accepted: 13 April 2023
Published: 19 April 2023

1. Introduction

In Serbia, as in other temperate climate countries, common bean has largely been grown under rainfed conditions. However, as a result of altered climatic conditions—corroborated by formal climate studies [1]—a dramatic decline in production of this staple food has been registered in Serbia over the past several decades, as well as lack of irrigation. The highest risk originates from increased air temperatures, erratic precipitation patterns and amounts, heat waves, frequent storm and hail events, increased number in dry and tropical days, etc. [2]. In addition, according to farmers' perception, climate change has a negative impact on plant production in Serbia [3]. Based on analyses of future climate scenarios in Southeast Europe through to the end of the century, air temperatures are expected to rise, dry periods are to lengthen, precipitation patterns will become increasingly non-uniform, and heat waves and other unwelcome events are to occur more often [4], implying the need to irrigate common bean. Countries poor in water resources, such as Serbia, need to develop irrigation strategies that meet the demands of various stakeholders. As such, the use of models for simulation of plant growth, water needs of crops, and water management will be increasingly important in the future for crop growth monitoring, forecasting of yield reduction in the event of drought, and allocating water to ensure profitable crop production. Many models have been developed to simulate plant growth or water management in agriculture, such as DSSAT, Cropsys, EPIC, APEX, WOFOS, SWAP, AquaCrop, etc. [5–9]. The models can be categorized into three types: energy-driven, carbon-driven, and water-driven. They can all be used in practice, with varying degrees of effectiveness [10]. As far as we are aware, DSSAT-BEANGRO has been calibrated to simulate common bean growth [7,11,12]. Recent research has dealt with the correlation between common bean (*Phaseolus vulgaris* L.) yield and irrigation water availability, providing irrigation water from higher elevations of a catchment to grow common bean at lower elevations in Haiti, using the Cropping System Model (CSM)-CROPGRO-Dry of DSSAT [13] or to optimize irrigation management as a function of the sowing date and the common bean cultivar [14].

Given that water would frequently be a growth-limiting factor in the future, the water-driven model, AquaCrop, has often been used in recent times because it is a robust model that requires only a limited number of input parameters, which can easily be measured in the field and is user friendly. Additionally, studies have shown that the model accurately simulates the yields and water requirements of various crops grown worldwide [15–19]. AquaCrop can also be used effectively to predict crop water requirements by assimilating the canopy cover estimated from Sentinel-2 imagery [20–23], and to evaluate the effects of optimized irrigation management on the minimization of percolation losses and maximization of crop yield for different soil types [24].

AquaCrop has been parameterized and validated for common bean growth simulation under Mediterranean climatic conditions (Davis, CA, USA), based on two experiment datasets from two doctoral theses, where common bean was grown with different irrigation treatments [25]. Some researchers have attempted to parameterize or calibrate AquaCrop for dry beans using the results of only a single experiment dataset in the tropical climatic condition of Cuba [26] or the megathermal and humid climate of Brazil [27,28]. AquaCrop can be used effectively to test sowing dates in the case of barley [29,30], sorghum [31], or sugar beet [32], and to optimize sowing dates in the case of sunflower and soybean [33]. Additionally, sowing date changes are proposed as a climate change impact mitigation measure. Studies show that spring sowing dates might be advanced, or aftercrop sowing dates delayed, due to unfavorable temperature conditions for the germination, growth, and development [34].

Given that no reports were found in the literature concerning the calibration of this model for temperate climates and common bean, or that AquaCrop can be used to effectively simulate sowing dates, the objectives of this research were to: (i) calibrate the AquaCrop model v.7.0 for temperate continental climatic conditions, (ii) simulate the yield of common bean in different growing periods and with various irrigation treatments, and (iii) test how reliably the model estimates irrigation water requirements that will ensure high productivity, which was a novel aspect of the research.

2. Materials and Methods

Relevant principles of the AquaCrop model are described in detail in [6,35]. In the present research, calibration was based on the default parameters of AquaCrop v.7.0 for common bean, as well as data collected during a two-year experiment on Chernozem soil in Syrmia (44°58′55.4″ N lat., 20°7′51.2″ E long.), in 2019 and 2020. The two-year experiment was of a two-factorial split-plot design, divided into subplots. The common bean cultivar was 'Sremac', a vertical bush bean variety with large leaves; its growing period is short, 70–90 days, and it tolerates drought and high temperatures in the flowering stage. Thus, the yields of this cultivar are stable in different climatic conditions. Three irrigation treatments were applied: F—full irrigation providing 100% of ETc (crop evapotranspiration), R—mild deficit irrigation at approximately 80% of ETc, and S—moderate deficit irrigation at approximately 60% of ETc. There were three sowing periods: standard I, mid-April, consistent with the climatic conditions in Serbia); late spring II, end of May/beginning of June; and summer III, third decade of June/beginning of July. The soil characteristics of the experimental site are described in detail in [36]. The climate input data (maximum and minimum air temperatures, maximum and minimum relative humidity, net radiation, wind velocity, and precipitation) were measured daily in the field by a micrometeorological station, and the data were validated against the nearest meteorological station of the first order in Surčin, at a distance of 20 km. The field file was based on measured canopy cover (CC) and soil water content data. The soil moisture was monitored by the standard gravimetric method, every seven to ten days. The soil was drilled and sampled by layer, at 0–20, 20–40, and 40–60 cm. The canopy cover sampling methods are described in detail in [36]. The yield and harvest index were recorded when the common bean was physiologically ripe and contained 10% of moisture. Table 1 shows the details of sowing and harvesting dates, irrigation depths, and amounts of precipitation.

Table 1. Sowing and harvesting dates with lengths of important growing phases of common bean and climatic characteristics during experiment.

Year	Treatment	Sowing Date	Length of Emergency/Leaf Development/Flowering/Pod Formation/Pod Maturation (Days)	Harvesting Date	Tm (°C)	Precipitation (mm)	Irrigation Depth (mm)
2019	F-I	22 April	16/29/9/25/15	25 July	25.22	430	0
	R-I						0
	S-I						0
	F-II	7 June	10/25/15/25/22	12 September	30.17	239	150
	R-II						117
	S-II						84
	F-III	3 July	7/26/12/26/21	3 October	28.12	171	249
	R-III						180
	S-III						129
2020	F-I	15 April	12/38/15/20/16	25 July	18.11	247	228
	R-I						162
	S-I						126
	F-II	28 May	9/33/16/19/21	3 September	22.00	314	141
	R-II						90
	S-II						75

For irrigation simulation, the model was set to three levels: (i) fulfill net irrigation demand (Fs) assuming option to start drip irrigation when 50% of readily available water (RAW) is depleted, and refill to nearly field capacity (−8 mm) for efficient use of rainfall, (ii) fulfill partial irrigation requirements Rs—start irrigation when 80% of RAW is depleted, and refill up to −20 mm of field capacity, and (iii) start irrigation when 100% of RAW is depleted and refill up to −25 mm (Ss). The simulated irrigation strategy was very close to that applied in the experiment, but it was not identical. The aim of this research was to assess the reliability of the model to be used for irrigation planning in a moderate climate, where irrigation is very often supplemental.

Calibration was based on local ground measured data on crop yield, biomass accumulation, canopy cover, soil moisture, irrigation depth, and evapotranspiration of common bean sown in the spring (as is standard practice in this part of Europe) and late spring, with full irrigation (I-F, II-F) and deficit irrigation treatments (II-R, II-S) in 2020. The other treatments in 2019 (I-F, II-F, III-F, II_R, III-R, II-S, III-S) and 2020 (I-R, I-S) were used for model validation. Treatments III-F, III-R, and III-S were excluded because invasion of forest bugs (*Pentatoma rufipes*) in the reproductive stage significantly lowered dry bean yields [37]. The growing degree day (GDD) option was selected, given that the growing cycle is shorter for the summer sowing date, compared to the other two. The observed GDD varied between 930, when the highest yield was obtained for the standard spring sowing date, and up to 1300 for the late spring sowing date, when the average yield of the fully irrigated common bean was obtained (Table 2). Calibration was based on the average GDD (Table 3), taking into account the duration of phenological stages (germination, leaf development, flowering, pod formation, senescence, and maturity). The average growing cycle lasted for 98, 94, and 100 days in sowing periods I, II, and III, respectively (Table 1). Iterations continued until good statistical parameters were achieved, as provided by the model based on observed and simulated values. Default parameters were taken for WP, crop coefficient, and the water stress.

Table 2. Growing degree days per growing cycle I (spring sowing period), II (late spring), and III (summer).

Year/Sowing Period	I	II	III	Average
2019	978	1300	1144	1141
2020	932	1226	-	1111

Table 3. Default and calibrated data, DAP—days after planting.

Parameter	Default	Calibrated
Canopy decline (CDC), % per day	0.881	1.104
Canopy expansion (CGC), % per day	11.8	9.7
Maximum canopy cover (CCx), %	99	95
GDD from DAP to emergence	59	98
GDD from DAP to maximum canopy	752	605
GDD from DAP to senescence	903	945
GDD to maturity	1298	1140
GDD from DAP to flowering	556	592
Flowering duration, GDD	233	206
Length building up harvest index (HI)	668	496
Maximum effective rooting depth, m	1.7	0.6
DGG from DAP to maximum root depth	888	449
Adjusted harvest index	40	50
Harvest index (Hlo), %	90	75

Five statistical methods were used to analyze and compare yield data derived from field experiments and simulations. The first was the root mean square error (*RMSE*) method and normalized *NRMSE*:

$$RMSE = \left[\sqrt{\frac{1}{n}\sum_{i=1}^{n}(S_i - M_i)^2}\right] \tag{1}$$

where S_i and M_i = simulated and measured values, respectively, and n = number of observations. The *RMSE* unit is the same for both variables (Mg·ha^{-1}), and the model's fit improves when *RMSE* tends toward zero, whereas the *NRMSE* unit is %.

$$NRMSE = \left[\sqrt{\frac{1}{n}\sum_{i=1}^{n}(S_i - M_i)^2}\right] \cdot \frac{100}{\overline{M}} \tag{2}$$

The second method was the mean bias error (MBE), which refers only to an error that is systematic in nature:

$$MBE = \left[\frac{1}{n}\sum_{i=1}^{n}(S_i - M_i)^2\right] \tag{3}$$

The index of agreement (d) was calculated using Equation (4) [38]:

$$d = 1 - \frac{\sum_{i=1}^{n}(S_i - M_i)^2}{\sum_{i=1}^{n}\left(|S_i - \overline{M}| + |M_i - \overline{M}|\right)^2} \tag{4}$$

where $\overline{M}$ = average values of measured data. The index of agreement d is a descriptor and its values range from 0 to 1. The model simulated the studied parameter better as the value approached 1.

The coefficient of determination R^2 is defined as the squared value of Pearson's correlation coefficient.

$$R^2 = \frac{\sum\left(Mi - \overline{M}\right)\left(Si - \overline{S}\right)}{\sqrt{\sum\left(Mi - \overline{M}\right)^2 \sum\left(Si - \overline{S}\right)^2}} \tag{5}$$

where $\overline{S}$ = average values of simulated data.

3. Results

The results of model calibration are shown in Table 4. It is apparent that the model estimated yields quite well, as the deviation ranged from 1.2% to −7.4%. The variation range of the estimated biomass was somewhat larger (3.7% to −14.9%). Based on all tested statistical indicators (*RMSE, NRMSE, MBE*, *d*, and R^2), there was an excellent agreement in the case of both yield and biomass (Table 5). The mean bias error (*MBE*) indicates the average bias of the prediction. *MBE* values were low, showing that the model was well calibrated and did not require further tuning. A negative *MBE* indicates that the model yields slightly lower values, whereas a positive *MBE* indicates that the total biomass is slightly higher. Figure 1 shows the seasonal trend of canopy cover and biomass accumulation for the calibrated dataset. The correlation between the observed and simulated CC and biomass was excellent, as corroborated by the statistical parameters computed by the model. The correlation coefficient varied from 0.91 to 0.99, *NRMSE* was <12% for CC and <25% for biomass, while the Willmott index *d* ranged from 0.92 to 0.99. The CC values derived via unmanned aerial vehicle (UAV), manual recording and calculations closely matched the simulated values, which will facilitate field data collection in the future.

Table 4. Simulation results of yield and biomass for calibration datasets of common bean (full (F) and deficit (R and S) irrigation treatments), obtained from two sowing periods, I (spring) and II (late spring) in 2020, and deviation from measured values.

Treatment	Measured	Simulated	Deviation	Measured	Simulated	Deviation
	Yield (Mg ha^{-1})		%	Biomass (Mg ha^{-1})		%
I-F	4.42	4.75	−7.4	8.6	9.49	−14.9
II-F	4.18	4.13	1.2	7.85	8.07	−2.8
II-R	3.92	3.71	5.4	7.77	7.48	3.7
II-S	3.5	3.25	7.1	7.24	6.82	5.8

Table 5. Statistical indices of yield and total biomass for calibration and validation datasets.

Variable	Calibration Dataset		Validation Dataset	
	Yield	Biomass	Yield	Biomass
RMSE (Mg·ha^{-1})	0.276	0.91	0.466	0.737
NRMSE (%)	6.89	11.64	12.09	9.87
MBE	−0.046	0.186	0.103	0.546
d	0.902	0.894	0.396	0.903
R^2	0.98	0.988	0.152	0.507

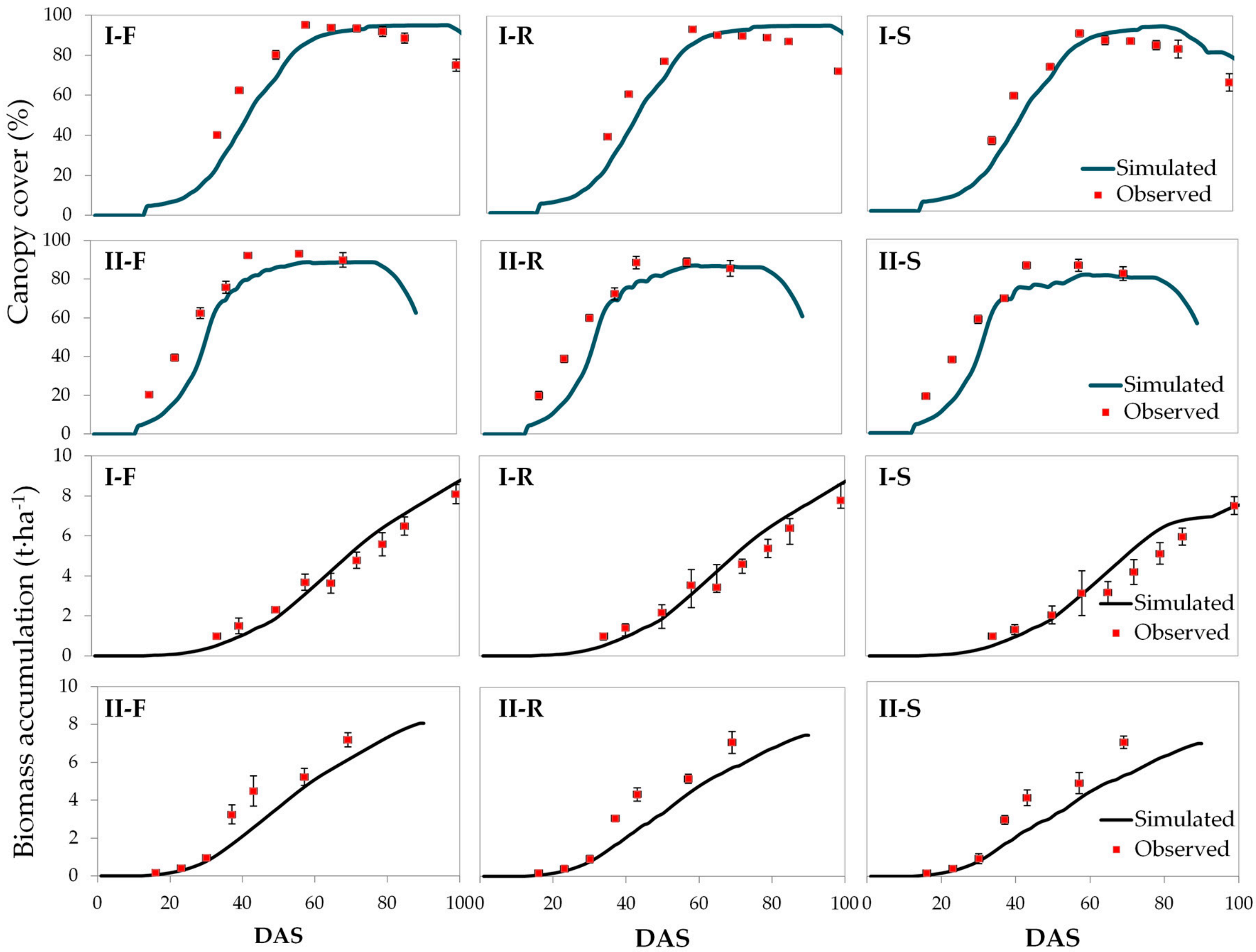

Figure 1. Simulation of canopy cover and biomass accumulation throughout the growing cycle of common bean used for model calibration per irrigation treatment; full (F) and deficit (R and S) irrigation treatments and sowing periods I (spring) and II (late spring).

The model validation results are shown in Table 6. The simulated yields deviated the least in the case of full irrigation, from −0.05% to 13.3%, and the most in the late sowing periods or high water-stress treatments (I-S, II-S, and III-S). The statistical indicators of the yield and final biomass simulations for the entire validation dataset showed an excellent agreement according to *NMRSE* (12.09% and 0.90%) and good to moderate agreement in the case of the other parameters (Table 5). A better agreement was achieved for biomass than yield. Low *MBE* values indicated that the model did not systemically distort the results. Figure 2 shows the simulated and observed CC data during the growing period, and Figure 3 the biomass accumulation data. The results indicate that most of the treatments achieved a very good match between the simulated and observed CC and biomass values. Somewhat larger deviations were noted in treatments II-S and III-S, at which time the common bean was exposed to a higher water stress and higher summer month temperatures. The statistical indicators computed by the model confirm good to excellent agreement for most of the treatments.

Table 6. Measured vs. simulated results for validation datasets of common bean grown under different water treatments; full (F) and deficit (R and S) irrigation and sowing period conditions I (spring), II (late spring), and III (summer).

Year	Treatment	Measured	Simulated	Deviation	Measured	Simulated	Deviation
		Yield (Mg ha^{-1})		%	Biomass (Mg ha^{-1})		%
2019	I-F	4.21	3.65	13.3	7.84	7.52	4.1
	II-F	3.84	3.95	−2.9	7.44	7.73	−3.9
	III-F	4.19	4.19	−0.05	8.07	8.14	−0.9
	II-R	3.75	3.92	−4.4	7.01	7.70	−9.8
	III-R	3.76	4.18	−11.1	7.4	8.11	−9.6
	II-S	3.27	3.79	−16.0	6.64	7.58	−14.2
	III-S	3.47	4.14	−19.3	7.05	8.05	−14.1
2020	I-R	4.26	4.62	−8.4	8.03	9.37	−16.7
	I-S	3.96	3.20	19.2	7.72	7.92	−2.5

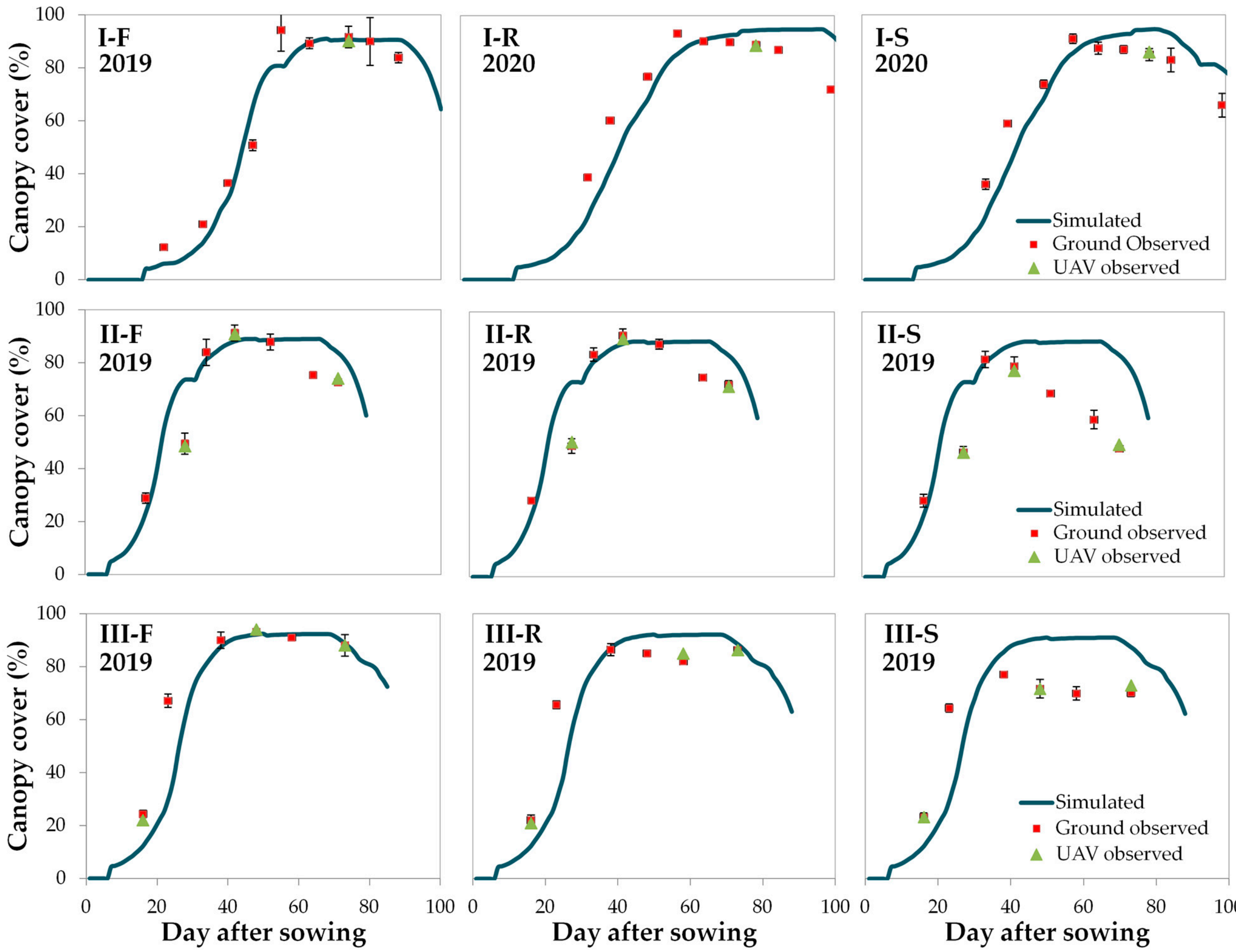

Figure 2. Simulated and observed canopy cover data during the growing period of the treatments used for model validation; full (F) and deficit (R and S) irrigation treatments and sowing periods I (spring), II (late spring), and III (summer).

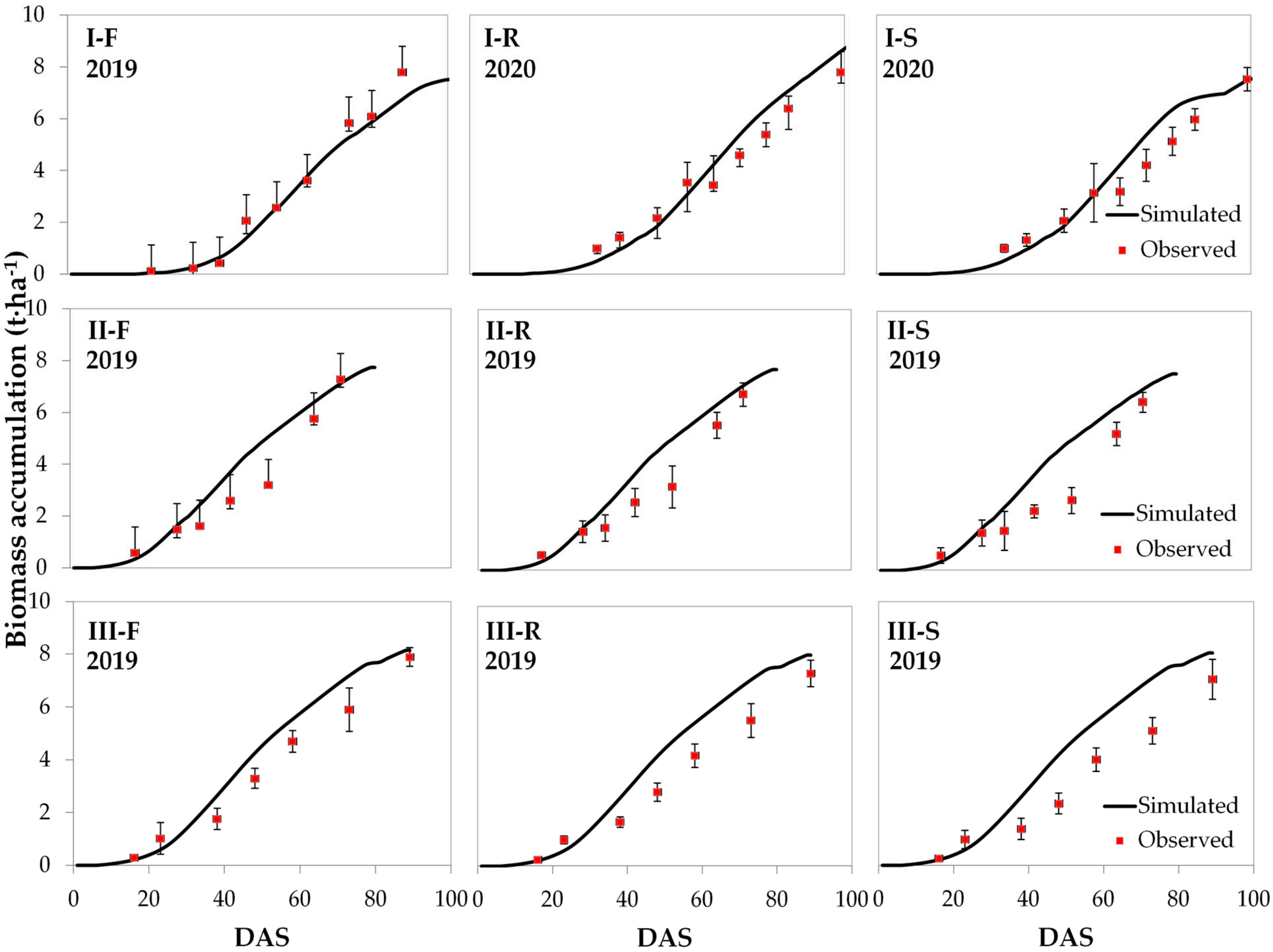

Figure 3. Simulated and observed data of biomass accumulation during the growing period of the treatments used for model validation; full (F) and deficit (R and S) irrigation treatments and sowing periods I (spring), II (late spring), and III (summer).

The model computed the irrigation norms for the full and two deficit irrigation treatments, based on the values set for the beginning of irrigation and the level to which the soil water reservoir needed to be refilled. Table 7 shows the average values. The model simulated only 29 mm, 32 mm, and 34 mm of more water for the Fs, Rs, and Ss irrigation strategies, compared to the actual amounts applied in the experiment. The deviations of the average values were larger in the case of the applied than the simulated norms. This was due to the adjustment of the beginning of irrigation to the occurrence and duration of rainfall, which the model could not identify; it recognized the daily precipitation total, but not whether rainfall lasted the entire day. Considering the yields achieved with these irrigation strategies, the model estimates were excellent in the case of full irrigation (Fs), since the deviations were from −0.8% to −9.3% (Table 8). The Rs deficit irrigation option resulted in a good agreement, with deviations ranging from −10.7% to 20.3%. The larger-deficit irrigation treatment (Ss) exhibited the poorest agreement, with deviations as high as 25%. Considering all irrigation options (Fs, Rs, and Ss) and sowing dates, the modeled yields were comparable to those achieved in the field. The statistical indicators showed that the model approximated well for the yields and irrigation norms (Table 9). It predicted a somewhat shorter growing period by about nine days. Taking all statistical indicators into account, the best results were achieved for total biomass, followed by yield. In the case of R^2, the descending order of agreement was growing cycle (GC), biomass (B), irrigation requirement (In), and yield (Y); for *NRMSE* it was Y, B, In, and GC; and for Willmott index *d* it was B, Y, GC, and In.

Table 7. Average applied and simulated irrigation norms In (mm) per irrigation treatment; full (F) and deficit (R and S) irrigation, including standard deviation.

Irrigation Treatment	Applied *In*	*SD*	Simulated *In*	*SD*
F	206	54	221	9
R	137	41	169	24
S	104	28	137	17

Table 8. Measured and simulated yields (Mg ha^{-1}) based on modeled irrigation depths; full (F) and deficit (R and S) irrigation treatments and sowing periods I (spring), II (late spring), and III (summer).

Treatment	Measured	Simulated	Deviation
I_F_2019	4.21	4.08	3.0
II_F_2019	3.84	4.13	−7.6
II_R_2019	3.75	4.10	−9.3
II_S_2019	3.27	4.10	−25.3
III_F_2019	4.19	4.22	−0.8
III_R_2019	3.76	4.20	−11.6
III_S_2019	3.47	4.10	−18.2
I_F_2020	4.42	4.75	−7.5
I_R_2020	4.26	4.72	−10.7
I_S_2020	3.96	4.53	−14.3
II_F_2020	4.18	4.20	−0.6
II_R_2020	3.92	4.72	−20.3
II_S_2020	3.5	4.17	−19.0

Table 9. Statistical indices of simulated irrigation norms, yield, total biomass, and growing cycle.

Variables	Yield (Y) (Mg ha^{-1})	Biomass (B) (Mg ha^{-1})	Irrigation Norms (*In*) (mm)	Growing Cycle (GC) (Days)
RMSE (Mg·ha^{-1})	0.161	0.33	15.06	10.5
NRMSE (%)	4.124	4.31	7.73	13.42
MBE	0.406	0.94	30.8	−8.8
d	0.64	0.78	−28.68	−11
R^2	0.56	0.73	0.66	0.84

4. Discussion

The AquaCrop model was calibrated for common bean and a temperate continental climate, where this crop is often both irrigated and rainfed. To better utilize the soil and extend the growing season, three sowing dates and three different levels of irrigation were applied, to determine the productive capability of a local common bean cultivar and arrive at the best irrigation strategy. Given that the model has a default file, in the first iteration all the conservative parameters were retained and only those characteristic of the farming technology were entered. However, the temperate continental climatic conditions required adjustment to reflect the actual GDD for the length of the growing cycle. Although the highest yields were achieved with the lowest GDD and longest growing cycle, averages were selected for all three growing dates in the two-year period. Additionally, changes were entered for the characteristics of the ‘Sremac’ common bean cultivar, including HI 50% [38] and water productivity (WP*) reduction at maturity to 75%, based on experimental data (not shown). Low *MBE* values show that the model does not systemically distort the results.

Considering the seasonal trends of CC and biomass accumulation, the results showed that most treatments achieved a very good agreement between the observed and simulated values. Somewhat larger deviations were noted in the treatments of the second and third sowing dates (S-II and S-III), when the common bean was exposed to a higher water stress and higher summer month temperatures. Similar findings are reported in [32]. Namely, the authors state that the deviation of the simulated from the observed CC values were also noted in the case of deep-rooted crops, such as sugar beet, where the model did not recognize the subtle significance of even low precipitation levels for root revitalization and delayed senescence, which increased the biomass and yield. Other researchers claim that the AquaCrop model predictions were less accurate in the case of the largest deficit irrigation treatments [10,39,40].

In the present research, the results obtained with the calibration dataset show that AquaCrop accurately predicted both biomass and yield, as corroborated by the results reported for common bean [26,27] and other crops under similar or different climatic and soil conditions [17,20,32]. Considering the validation dataset, the model predicted the yield and biomass better when there was no water stress. Such findings were also reported by Espandafor et al. [25], who state that the best simulation results were achieved with well-irrigated or non-irrigated common bean. Katerji et al. [16] obtained higher deviations of yield and biomass of tomato grown in no-water stress conditions and under mild stress, from 4.2% up to 16.7%, respectively, which is consistent with the present research, where the variation was from -0.05 to 19.3%. Although the model is complex and comprehensive with regard to the plant response to water, it cannot recognize local conditions, such as the duration of rainfall and the occurrence of heavy dew, which reduce water stress, or a protracted fog event which extends the growing cycle. This is why the model yielded higher deviation results in the case of treatments R and S, and sowing dates II and III in comparison to F treatments. The length of the common bean growing cycle depends on GDD, but some phenological stages also require a certain photoperiod because the estimated and observed growing cycles were not closely matched. Namely, in the case of the spring sowing date (I), the model extended the growing period by 4-5 days and shortened it for growing periods II and III by 14 and 4 days, respectively. This might have been caused by biomass and yield estimation errors. Based on the statistical indicators, the model approximated soil moisture fairly (data not shown). It generally provided values higher than observed, occasionally lower, possibly due to the sampling procedure associated with drip irrigation. An error might also occur because the model considers runoff and deep percolation, but not interceptions on the leaves, and might overestimate the soil water content. This is expected more often when rainfall events occur frequently with low depths, which was the case in this experiment. Statistical indices for the calibration dataset obtained by the model showed a strong correlation between the measured and simulated soil water content according to Pearson correlation coefficient $r > 0.8$, and moderate agreement according to *NRMSE* (15.9–20.9%) and d (0.54–0.72). The results obtained for the validation data set indicated a moderate correlation (r varied from 0.41–0.8), with an *NRMSE* of 10–30.1%, and d varying from 0.46 to 0.72. In the same experiment, a strong correlation was noted between the normalized difference vegetation index (NDVI) and CC, leaf area index and transpiration, and a weak and negative correlation with soil moisture [36]. A sample collected close to a drip will certainly exhibit a higher soil moisture. Other reports also state that the model does not offer good soil moisture simulation results. For example, Cheng et al. [19] claim that AquaCrop overestimated SWC of cherry tomato grown in a greenhouse under plastic mulch. Similarly, Ćosić et al. [18] reported that a good agreement between simulated and observed SWC values is not always achieved. They indicate that a good agreement was noted at the beginning and towards the end of the growing season. There were considerable deviations in the middle of the period. This is consistent with our findings.

Testing of the model with regard to the determination of irrigation strategies for several sowing dates revealed that it estimated well for the water requirements of common bean and that the yields were high. According to *NRMSE*, the deviation of the estimated irrigation norms for all three strategies was 7.7% and that of yield even less, 4.31%. The statistical indicators showed that AquaCrop can be used to schedule irrigation of common bean grown during multiple sowing periods. Similar findings and observations are reported in [32], after testing of the model for several sowing dates and different climatic conditions in the case of sugar beet. Namely, the researchers conclude that AquaCrop can be a useful tool to determine the irrigation water allocation strategy to achieve high water productivity of sugar beet, taking into account the impact of seasonal rainfall and water saving. Consequently, in a temperate continental climate AquaCrop estimates irrigation needs well, where irrigation is often supplemental to rainfall for spring sowing dates. A number of papers conclude that AquaCrop can be used effectively to determine the optimal irrigation norms for various sowing dates, including Araja [31] for sorghum, Martínez-Romero [40] for barley, Li [41] for cotton and Huang [42] for wheat.

5. Conclusions

The results of this study confirm that the AquaCrop model can be used to estimate the seasonal pattern of canopy cover, biomass, and yield of field beans grown under three different water supply conditions and in three sowing periods. Some deviation of simulated from measured data was observed in the deficit irrigation treatments (R and S) in the late spring seeding period. The model underestimated the length of the growing season by up to 9 days but predicted yield and total biomass very well. For multiple irrigation strategies, the model estimated yields for full irrigation (Fs) with deviations ranging from −0.8% to −9.3%. In the case of deficit irrigation Rs, the agreement with observed values was good. A larger deviation was noted in the case of deficit irrigation Ss. Considering all the irrigation simulation options (Fs, Rs, and Ss) and sowing dates, the simulated yields corresponded to those observed in the field. The conclusion of this research is that the model is reliable for agricultural water management of common bean in temperate climates.

Author Contributions: Conceptualization, R.S.; methodology, R.S. and M.Ć.; investigation, A.L. and M.Ć.; resources, N.D.; data curation, A.L. and R.S.; writing—original draft preparation, R.S.; writing—review and editing, A.L. and R.S.; visualization, A.L. and D.S.; supervision, N.D. and D.S. All authors have read and agreed to the published version of the manuscript.

Funding: This paper was produced within the scope of project 451-03-68/2022-14/200116 funded by the Serbian Ministry of Education, Science and Technological Development.

Data Availability Statement: Not applicable.

Acknowledgments: The authors would like to thank the company Napredak A.D. from Stara Pazova for providing their experimental field for this study. This work was prepared within the framework of project 451-03-47/2023-01/200116 funded by the Serbian Ministry of Education, Science and Technological Development.

Conflicts of Interest: The authors declare no conflict of interest.

References

1. Vukovic, A.; Vujadinovic, M.; Rendulic, S.; Djurdjevic, V.; Ruml, M.; Babic, V.; Popovic, D. Global Warming Impact on Climate Change in Serbia for the Period 1961–2100. *Therm. Sci.* **2018**, *2018*, 2267–2280. [CrossRef]
2. Mandic, M.V.; Vimic, A.V.; RankovicVasic, Z.; Đurovic, D.; COsic, M.; Sotonica, D.; Nikolic, D.; Đurdevic, V. Observed Changes in Climate Conditions and Weather-Related Risks in Fruit and Grape Production in Serbia. *Atmosphere* **2022**, *13*, 948. [CrossRef]
3. Stricevic, R.J.; Lipovac, A.D.; Prodanovic, S.A.; Ristovski, M.A.; Petrovic Obradovic, O.T.; Durovic, N.L.J.; Durovic, D.B. Vulnerability of Agriculture to Climate Change in Serbia—Farmers' Assessment of Impacts and Damages. *J. Agric. Sci.* **2020**, *65*, 263–281. [CrossRef]
4. Nistor, M.M.; Ronchetti, F.; Corsini, A.; Cheval, S.; Dumitrescu, A.; Rai, P.K.; Petrea, D.; Dezsi, Ş. Crop Evapotranspiration Variation under Climate Change in Southeast Europe during 1991–2050. *Carpathian J. Earth Environ. Sci.* **2017**, *12*, 571–582.
5. Boogaard, H.L.; van Diepen, C.A.; Rotter, R.P.; Cabrera, J.M.C.A.; van Laar, H.H. *User's Guide for the WOFOST 7.1 Crop Growth Simulation Model and WOFOST Control Center 1.5*; Technical Document 52; DLO-Winand Staring Centre: Wageningen, The Netherlands, 1998.
6. Raes, D.; Steduto, P.; Hsiao, T.C.; Fereres, E. AquaCrop—The FAO Crop Model to Simulate Yield Response to Water: II. Main Algorithms and Software Description. *Agron. J.* **2009**, *101*, 438–477. [CrossRef]
7. Hoogenboom, G.; Porter, C.H.; Boote, K.J.; Shelia, V.; Wilkens, P.W.; Singh, U.; White, J.W.; Asseng, S.; Lizaso, J.I.; Moreno, L.P.; et al. The DSSAT crop modeling ecosystem. In *Advances in Crop Modeling for a Sustainable Agriculture*; Boote, K.J., Ed.; Burleigh Dodds Science Publishing: Cambridge, UK, 2019; pp. 173–216. [CrossRef]

8. Wang, X.; Kemanian, A.; Williams, J.R. Special features of the EPIC and APEX modeling package and procedures for parameterization, calibration, validation, and applications. In *Methods of Introducing System Models into Agricultural Research*; Ahuja, L.R., Ma, L., Eds.; Advances in Agricultural Systems Modeling 2; Wiley: Hoboken, NJ, USA, 2011; pp. 177–208.
9. Kroes, J.G.; van Dam, J.C.; Bartholomeus, R.P.; Groenendijk, P.; Heinen, M.; Hendriks, R.F.A.; Mulder, H.M.; Supit, I.; van Walsum, P.E.V. *SWAP Version 4; Theory Description and User Manual*; Report 2780; Wageningen Environmental Research: Wageningen, The Netherlands, 2017; Available online: https://library.wur.nl/WebQuery/wurpubs/fulltext/416321 (accessed on 27 January 2023).
10. Todorovic, M.; Albrizio, R.; Zivotic, L.; Abi Saab, M.T.; Stöckle, C.; Steduto, P. Assessment of AquaCrop, Cropsyst, and WOFOST Models in the Simulation of Sunflower Growth under Different Water Regimes. *Agron. J.* **2009**, *101*, 509–521. [CrossRef]
11. Jones, J.W.; Hoogenboom, G.; Porter, C.H.; Boote, K.J.; Batchelor, W.D.; Hunt, L.A.; Wilkens, P.W.; Singh, U.; Gijsman, A.J.; Ritchie, J.T. The DSSAT cropping system model. *Eur. J. Agron.* **2003**, *18*, 235–265. [CrossRef]
12. Oliveira, E.C.D.; Costa, J.M.N.D.; Paula Júnior, T.J.D.; Ferreira, W.P.M.; Justino, F.B.; Neves, L.D.O. The performance of the CROPGRO model for bean (*Phaseolus vulgaris L.*) yield simulation. *Acta Sci. Agron.* **2012**, *34*, 239–246. [CrossRef]
13. Mompremier, R.; Her, Y.; Hoogenboom, G.; Migliaccio, K.; Muñoz-Carpena, R.; Brym, Z.; Colbert, R.W.; Jeune, W. Modeling the Response of Dry Bean Yield to Irrigation Water Availability Controlled by Watershed Hydrology. *Agric. Water Manag.* **2021**, *243*, 106429. [CrossRef]
14. Coelho, A.P.; Faria, R.T.; de Lemos, L.B.; Cazuza Neto, A. Application of the CSM-CROPGRO-Dry Bean Model to Optimize Irrigation as a Function of Sowing Date in Common Bean Cultivars. *Field. Crop. Res.* **2023**, *293*, 108840. [CrossRef]
15. Stricevic, R.; Cosic, M.; Djurovic, N.; Pejic, B.; Maksimovic, L. Assessment of the FAO AquaCrop Model in the Simulation of Rainfed and Supplementally Irrigated Maize, Sugar Beet and Sunflower. *Agric. Water Manag.* **2011**, *98*, 1615–1621. [CrossRef]
16. Katerji, N.; Campi, P.; Mastrorilli, M. Productivity, Evapotranspiration, and Water Use Efficiency of Corn and Tomato Crops Simulated by AquaCrop under Contrasting Water Stress Conditions in the Mediterranean Region. *Agric. Water Manag.* **2013**, *130*, 14–26. [CrossRef]
17. Linker, R.; Ioslovich, I.; Sylaios, G.; Plauborg, F.; Battilani, A. Optimal Model-Based Deficit Irrigation Scheduling Using AquaCrop: A Simulation Study with Cotton, Potato and Tomato. *Agric. Water Manag.* **2016**, *163*, 236–243. [CrossRef]
18. Ćosić, M.; Stričević, R.; Djurović, N.; Moravčević, D.; Pavlović, M.; Todorović, M. Predicting Biomass and Yield of Sweet Pepper Grown with and without Plastic Film Mulching under Different Water Supply and Weather Conditions. *Agric. Water Manag.* **2017**, *188*, 91–100. [CrossRef]
19. Cheng, M.; Wang, H.; Fan, J.; Xiang, Y.; Liu, X.; Liao, Z.; Abdelghany, A.E.; Zhang, F.; Li, Z. Evaluation of AquaCrop Model for Greenhouse Cherry Tomato with Plastic Film Mulch under Various Water and Nitrogen Supplies. *Agric. Water Manag.* **2022**, *274*, 107949. [CrossRef]
20. Marta, A.D.; Chirico, G.B.; Bolognesi, S.F.; Mancini, M.; D'Urso, G.; Orlandini, S.; De Michele, C.; Altobelli, F. Integrating Sentinel-2 Imagery with AquaCrop for Dynamic Assessment of Tomato Water Requirements in Southern Italy. *Agronomy* **2019**, *9*, 404. [CrossRef]
21. Abi Saab, M.T.; El Alam, R.; Jomaa, I.; Skaf, S.; Fahed, S.; Albrizio, R.; Todorovic, M. Coupling remote sensing data and AquaCrop model for simulation of winter wheat growth under rainfed and irrigated conditions in a Mediterranean environment. *Agronomy* **2021**, *11*, 2265. [CrossRef]
22. Han, C.; Zhang, B.; Chen, H.; Liu, Y.; Wei, Z. Novel approach of upscaling the FAO AquaCrop model into regional scale by using distributed crop parameters derived from remote sensing data. *Agric. Water Manag.* **2020**, *240*, 106288. [CrossRef]
23. Jin, X.; Li, Z.; Feng, H.; Ren, Z.; Li, S. Estimation of maize yield by assimilating biomass and canopy cover derived from hyperspectral data into the AquaCrop model. *Agric. Water Manag.* **2020**, *227*, 105846. [CrossRef]
24. Corbari, C.; Ben Charfi, I.; Mancini, M. Optimizing Irrigation Water Use Efficiency for Tomato and Maize Fields across Italy Combining Remote Sensing Data and the AquaCrop Model. *Hydrology* **2021**, *8*, 39. [CrossRef]
25. Espadafor, M.; Couto, L.; Resende, M.; Henderson, D.W.; Garcia-Vila, M.; Fereres, E. Simulation of the Responses of Dry Beans (*Phaseolus vulgaris L.*) to Irrigation. *Trans. ASABE* **2017**, *60*, 1983–1994. [CrossRef]
26. Olivera, M.S.N.T.; Manrique, C.O.B.; Masjuan, M.S.Y.G.; Alega, I.A.M.G. Evaluation of AquaCrop model in crop dry bean growth simulation. *Rev. Cienc. Técnicas Agropecu.* **2016**, *25*, 23–30. [CrossRef]
27. Costa, M.S.; Mantovani, E.C.; Aleman, C.C.; Cunha, F.F. Using AquaCrop for crop bean according to different depth irrigation. In Proceedings of the IV Inovagri International Meeting, XXVI National Congress on Irrigation and Drainage and III Brazilian Symposium on Salinity, Fortaleza, Brazil, 2–6 October 2017.
28. Magalhães, I.D.; Lyra, G.B.; de Souza, J.L.; Teodoro, I.; da Rocha, A.E.Q.; Cavalcante, C.A., Jr.; Lyra, G.B.; Ferreira, R.A., Jr.; de Carvalho, A.L.; Ferraz, R.L.; et al. Performance of the AquaCrop Model for Bean (*Phaseolus vulgaris L.*) under Irrigation Condition. *Aust. J. Crop Sci.* **2019**, *13*, 1188–1196. [CrossRef]
29. Araya, A.; Habtu, S.; Hadgu, K.M.; Kebede, A.; Dejene, T. Test of AquaCrop Model in Simulating Biomass and Yield of Water Deficient and Irrigated Barley (*Hordeum vulgare*). *Agric. Water Manag.* **2010**, *97*, 1838–1846. [CrossRef]
30. Abrha, B.; Delbecque, N.; Raes, D.; Tsegay, A.; Todorovic, M.; Heng, L.; Vanutrecht, E.; Geerts, S.; Garcia-Vila, M.; Deckers, S. Sowing Strategies for Barley (*Hordeum vulgare* L.) Based on Modelled Yield Response to Water with AquaCrop. *Exp. Agric.* **2012**, *48*, 252–271. [CrossRef]
31. Araya, A.; Kisekka, I.; Holman, J. Evaluating Deficit Irrigation Management Strategies for Grain Sorghum Using AquaCrop. *Irrig. Sci.* **2016**, *34*, 465–481. [CrossRef]

32. Garcia-Vila, M.; Morillo-Velarde, R.; Fereres, E. Modeling Sugar Beet Responses to Irrigation with AquaCrop for Optimizing Water Allocation. *Water* **2019**, *11*, 1918. [CrossRef]
33. Abi Saab, M.T.; Albrizio, R.; Nangia, V.; Karam, F.; Rouphael, Y. Developing scenarios to assess sunflower and soybean yield under different sowing dates and water regimes in the Bekaa valley (Lebanon): Simulations with AquaCrop. *Int. J. Plant Prod.* **2014**, *8*, 457–482.
34. Stricevic, R.J.; Stojakovic, N.; Vujadinovic-Mandic, M.; Todorovic, M. Impact of Climate Change on Yield, Irrigation Requirements and Water Productivity of Maize Cultivated under the Moderate Continental Climate of Bosnia and Herzegovina. *J. Agric. Sci.* **2018**, *156*, 618–627. [CrossRef]
35. Steduto, P.; Hsiao, T.C.; Fereres, E.; Raes, D. *Crop Yield Response to Water. Irrigation and Drainage Paper*; No. 66; FAO: Rome, Italy, 2012; pp. 16–49.
36. Lipovac, A.; Bezdan, A.; Moravčević, D.; Djurović, N.; Ćosić, M.; Benka, P.; Stričević, R. Correlation between Ground Measurements and UAV Sensed Vegetation Indices for Yield Prediction of Common Bean Grown under Different Irrigation Treatments and Sowing Periods. *Water* **2022**, *14*, 3786. [CrossRef]
37. Willmott, C.J. Some Comments on the Evaluation of Model Performance. *Bull. Am. Meteorol. Soc.* **1982**, *63*, 1309–1313. [CrossRef]
38. Stajković-Srbinović, O.; Delić, D.; Kuzmanović, Đ.; Rasulić, N.; Tomić, Z. Common bean (*Phaseolus vulgaris* L.) growth promotion as affected by co-inoculation with rhizobium and rhizobacteria. In Proceedings of the 4th International Congress New Perspectives and Challenges of Sustainable Livestock Production, Belgrade, Serbia, 7–9 October 2015; pp. 803–810.
39. Alishiri, R.; Paknejad, F.; Aghayari, F. Simulation of Sugarbeet Growth under Different Water Regimes and Nitrogen Levels by AquaCrop. *Int. J. Biosci.* **2014**, *4*, 1–9. [CrossRef]
40. Martínez-Romero, A.; López-Urrea, R.; Montoya, F.; Pardo, J.J.; Domínguez, A. Optimization of Irrigation Scheduling for Barley Crop, Combining AquaCrop and MOPECO Models to Simulate Various Water-Deficit Regimes. *Agric. Water Manag.* **2021**, *258*, 107219. [CrossRef]
41. Li, F.; Yu, D.; Zhao, Y. Irrigation Scheduling Optimization for Cotton Based on the AquaCrop Model. *Water Resour. Manag.* **2019**, *33*, 39–55. [CrossRef]
42. Huang, M.; Wang, C.; Qi, W.; Zhang, Z.; Xu, H. Modelling the Integrated Strategies of Deficit Irrigation, Nitrogen Fertilization, and Biochar Addition for Winter Wheat by AquaCrop Based on a Two-Year Field Study. *Field Crop. Res.* **2022**, *282*, 108510. [CrossRef]